

# Kinetic Studies of Photocatalytic Degradation in a TiO<sub>2</sub> Slurry System: Distinguishing Working Regimes and Determining Rate Dependences

Kanheya Mehrotra, Gregory S. Yablonsky,<sup>†</sup> and Ajay K. Ray\*

Department of Chemical and Environmental Engineering, National University of Singapore, 10 Kent Ridge Crescent, Singapore 119260, Singapore

A systematic analysis has been carried out to distinguish “kinetic” and “transport” limited regimes for photocatalytic degradation in a TiO<sub>2</sub> slurry system using benzoic acid as a model component. Experiments were performed to investigate the effect of both monoparametric (e.g., catalyst loading, circulation rate, and initial concentration) and biparametric (e.g., catalyst loading and circulation rate, initial concentration of solute, and light intensity) on the degradation rate to differentiate the kinetic regime from the transport regime. It is shown that there is no external mass-transfer limitation at any catalyst loading, but at high catalyst loading, there exist both internal mass-transfer limitation and light limitation. The domain of kinetic limitation, the domain of internal mass-transfer limitation (particle agglomeration effect), and the domain of light transport limitation (shielding effect) were distinguished. Experimental results demonstrate a significant difference in the rate values between the “optimal catalyst loading” regime and the kinetic regime. The true kinetic dependences of the photocatalytic degradation rate on light intensity and the substance initial concentration were determined.

## Introduction

Wastewater treatment by low-energy UV-irradiated titanium dioxide, generally known as heterogeneous photocatalysis, has great potential as an alternative method for water purification and has become a subject of increasing interest over the last 15 years. The potential of this new technique has attracted numerous researchers to work in this area.<sup>1–7</sup> The first clear recognition and implementation of photocatalysis as a method of water purification was conducted by Ollis and co-workers<sup>4–7</sup> in the photomineralization of halogenated hydrocarbon contaminants in water, including trichloroethylene, dichloromethane, chloroform, and carbon tetrachloride, sensitized by TiO<sub>2</sub>. Since then, numerous studies<sup>8–12</sup> have shown that a great variety of dissolved organic compounds could be oxidized to CO<sub>2</sub> by a heterogeneous photocatalysis technique. Many reviews<sup>13–19</sup> have also been devoted to this area of research. In the review article,<sup>18</sup> more than 1200 references on the subject have been reported and an exhaustive list of chemicals that can be treated by a heterogeneous photocatalysis process has also been provided.

The reason for this immense attraction is the number of advantages this process has over the traditional methods and other advanced oxidation processes of water treatment, particularly, the following: (a) there is complete mineralization of many organic pollutants to environmentally benign effluents such as carbon dioxide, water, and mineral acid; (b) in general, there is no need for the use of expensive and dangerous oxidizing chemicals (such as O<sub>3</sub> or H<sub>2</sub>O<sub>2</sub>) because dissolved oxygen (or air) is sufficient; (c) TiO<sub>2</sub> as a

catalyst is active, inexpensive, nonhazardous, stable, and reusable; (d) the light required to activate the catalyst is low-energy UV-A, and it is also possible to use solar light as an alternative.

The mechanism of a photocatalysis reaction has been discussed in many books<sup>20–22</sup> and papers.<sup>23,24</sup> The individual steps that drive the above reaction are still not well understood because of the complex processes involved. The semiconductor photocatalytic oxidation of organic species dissolved in water by gaseous oxygen poses a number of questions with respect to the three-phase system and its interaction with light. It can, therefore, be referred to as a “four-phase” system, with the fourth phase being the “UV light–electronic” phase. These questions pose a great challenge, and the first step of the investigation must be a systematic study and understanding of the macrokinetic factors affecting the photocatalytic degradation rate.

## Macrokinetic Studies

Many macrokinetic studies have been done to date to understand the effects of various parameters in the degradation of compounds through heterogeneous photocatalysis. The past works<sup>23,25–27</sup> have analyzed various macrokinetic factors, namely, (a) catalyst loading, (b) initial concentration of the solute, (c) light intensity, (d) circulation rate, (e) pH of the solution, (f) partial pressure of oxygen, and (g) temperature, which affect the degradation rate (see Table 1). The following general conclusions can be drawn from the past macrokinetic studies.

1. The reaction rate depends on the initial concentration of the solute. Although at high concentration the observed rate is independent of the solute concentration (zeroth-order dependence), at low concentration it shows first-order dependence, while at some intermediate concentration it follows Langmuir-type dependence.<sup>2</sup>

\* To whom correspondence should be addressed. Fax: + 65 6779 1936. E-mail: cheakr@nus.edu.sg.

<sup>†</sup> Present address: Department of Chemical Engineering, Washington University, St. Louis, MO.

**Table 1. Important Macrokinetic Factors Affecting the Photocatalytic Degradation Rate As Reported by a Few Investigators in the Open Literature**

investigators	Chen and Ray <sup>27</sup>	Rideh et al. <sup>26</sup>	Inel and Okte <sup>23</sup>	Matthews <sup>11</sup>
pollutant	4-nitrophenol	2-chlorophenol	malonic acid	phenol, 4-chlorophenol, benzoic acid
experimental setup	swirl-flow reactor with a suspended catalyst and recirculation	cylindrical annular Pyrex reactor with external recirculation	annulus reactor with a pump to recirculate the suspension	spiral reactor, with a pump to recirculate the suspension
macrokinetic factors	results			
1 initial concentration	initial observed rate is pseudo-first-order with respect to the initial concentration	rate decreases with an increase of the initial concentration	rate increases and reaches a plateau at high concentration; Langmuir-type dependence	rate is zero-order at high concentration and first-order at low concentration
2 catalyst loading	rate increases and reaches a plateau at a catalyst loading of 2 g/L	rate increases and reaches a plateau at a catalyst loading of 0.2 g/L	rate increases and reaches a plateau at a catalyst loading of 1 g/L	at low solute concentration, the lowest loading gives a greater rate at high solute concentration
3 light intensity	rate $\propto I^\beta$ , where $\beta$ is between 0.5 and 1.0	rate is proportional to the light intensity	rate $\propto I^{0.5}$	not studied
4 circulation rate	not studied	not studied	rate increases with the circulation rate and reaches a plateau	no significant effect of the circulation rate and assumed no mass-transfer limitation
5 pH	at both high and low pH values, the degradation rate is quite slow; the best pH is near pzc, i.e., between 5.6 and 6.4	low rate in the acidic region, constant rate in the neutral region, and increasing rate in the basic region	rate increases with pH and reaches a plateau at pH = 9 surface charge of TiO <sub>2</sub> is strongly influenced by pH	not studied
6 partial pressure of oxygen, $P_{O_2}$	rate increases with $P_{O_2}$ and reaches a plateau at about 0.4 atm	rate increases nonlinearly with $P_{O_2}$	not studied	not studied
7 temperature	not significant	not significant	rate increases with $T$	not studied

2. The reaction rate increases with catalyst loading, reaches a maximum at some optimum catalyst loading, and then decreases. The researchers attribute the decrease of rate at high catalyst loading to the obstruction of light transmission and defined it as the "shielding effect".<sup>28</sup>

3. The reaction rate is proportional to the light intensity, but at higher intensities the rate becomes proportional to the square root of the light intensity. It is explained that, as the light intensity increases, so does the recombination rate of hole and electron.<sup>29</sup>

4. The effect of the circulation rate on the degradation rate has also been studied. Typically, no influence of the circulation rate on the degradation rate has been found in slurry systems,<sup>25,27</sup> although an increase in the degradation rate due to the circulation rate has been reported in ref 23.

5. In most cases, it is found that pH has a direct impact on the degradation rate. It has been observed that the pH affects the surface properties of the TiO<sub>2</sub> catalyst, and hence the degradation rate gets affected.<sup>30</sup>

6. The rate increases with the increase of oxygen partial pressure. The typical explanation is that oxygen acts as an electron scavenger, thus reducing the rate of electron-hole recombination.<sup>31</sup>

7. The effect of temperature is not so significant within the studied interval, probably because of the countereffect of a decrease in the adsorption constant of solute on the catalyst.<sup>27</sup>

One of the most important issues of macrokinetic studies is distinguishing the "kinetic" region in which the observed rate is governed by kinetic dependences. Obviously, intrinsic kinetic data are necessary for catalyst characterization and reactor design. Traditionally, in the kinetic studies of heterogeneous catalysis,

to distinguish the kinetic regime from the "transport-limited" regime, data related to the substance transformation over catalyst must be presented using the dependence mole per unit mass of catalyst per unit time instead of mole per unit volume of solution per unit time. This kind of data representation with the dimension of rate of reaction based on per unit mass of catalyst can be found in the literature of multiphase slurry reactions with a suspended catalyst (e.g., in ref 32). However, in the literature devoted to the photocatalytic degradation of organic solutes such a representation of data is not a common feature. Typically, kinetic data are presented using the dimension of mole per unit volume of solution per unit time and the kinetic region, rigorously to say, cannot be identified. Also, in the open literature the experimental data are most commonly presented only for monoparametric studies, in which the influence of only one parameter (such as catalyst loading, light intensity, initial concentration, etc.) on the reaction rate is studied. There are very few studies<sup>32</sup> related to the combined effect of the simultaneous change of different parameters on the reaction rate (such as catalyst loading and circulation rate, initial concentration and light intensity, etc.). Evidently, there is a need to do special detailed experiments using both monoparametric and biparametric studies to reveal the kinetic regime and analyzing the influence of many above-mentioned factors on the observed degradation rate of the process.

The aim of this work is to provide a more systematic analysis of the effect of important macrokinetic parameters on the degradation rate of benzoic acid, which has been chosen in this study as the model compound. Experiments were conducted to investigate the effect of the above-mentioned single parameter and the si-

multaneous effect of two parameters on the photocatalytic degradation rate of benzoic acid. The expected results of the studies are (a) distinguishing the kinetic regime from the transport limitation regime [in a photocatalytic process, transport limitation could be governed by either substance (pollutant) transport (external and/or internal) or light transport] and (b) experimental analysis of the rate dependences on the reaction parameters (substance concentration and light intensity).

## Experimental Details

**Experimental Setup.** The photocatalytic degradation of benzoic acid was investigated in aqueous suspensions of a  $\text{TiO}_2$  catalyst. The apparatus is comprised of a photocatalytic reactor, UV lamp, peristaltic pump, water bath, and gas flowmeter. All experiments were conducted in a semibatch swirl-flow monolithic-type photoreactor. The semibatch reactor consisted of two circular glass plates (each of diameter 0.09 m) separated by 0.01 m, which were placed between soft padding housed within stainless steel and aluminum casings. Pyrex glass plates were used because they can cut off UV light below 300 nm, thereby eliminating direct photolysis of the organic compounds. The volume of the reactor used was 63.5 mL. The reaction solution, which was circulated by a peristaltic pump, was introduced tangentially between the two glass plates and exited from the center of the top plate. The tangential introduction of liquid created a swirl flow, thereby ensuring that the liquid solution was well mixed.<sup>2</sup> The above reactor was connected to a Perkin-Elmer UV spectrophotometer for online measurement of benzoic acid. A lamp (Philips HPR 125 W high-pressure mercury vapor) was placed about 0.1 m underneath the bottom glass plate on a holder that could be moved to create a different angle of incidence of light. The lamp has a spectral energy distribution with a sharp (primary) peak at  $\lambda = 365 \text{ nm}$  of 2.1 W with an incident light intensity of  $213 \text{ W/m}^2$ . The light intensity was measured by a digital radiometer (model UVX-36; UVP). A provision was made for placement of several metal screens of different mesh sizes between the lamp and the bottom glass plate to obtain variation in the light intensity. The lamp and reactor were placed inside a wooden box painted black so that no stray light can enter the reactor. The lamp was constantly cooled by compressed air to keep the temperature down, thereby protecting the lamp from overheating. Teflon tubing was used to connect the reactor and the beaker. The schematic diagram of the experiment setup is shown in Figure 1 while the photoreactor is shown in Figure 2.

A Degussa P25 catalyst provided by Degussa Company (Germany) was used throughout this work without further modification. Its main physical data are as follows: Brunauer–Emmett–Teller surface area,  $55 \pm 15 \text{ m}^2/\text{g}$ ; average primary particle size, around 30 nm; purity, above 97%; anatase/rutile, 80:20. Benzoic acid (99.5+%) was obtained from BDH Chemicals. All chemicals were used as received. Benzoic acid was chosen as the model compound because it can be measured easily and accurately by a spectrophotometer. Water used in this work was always Millipore water (from a Milli Q plus185 ultrapure water system).

A Shimadzu 5000A total organic carbon (TOC) analyzer with an ASI-5000 autosampler was used to

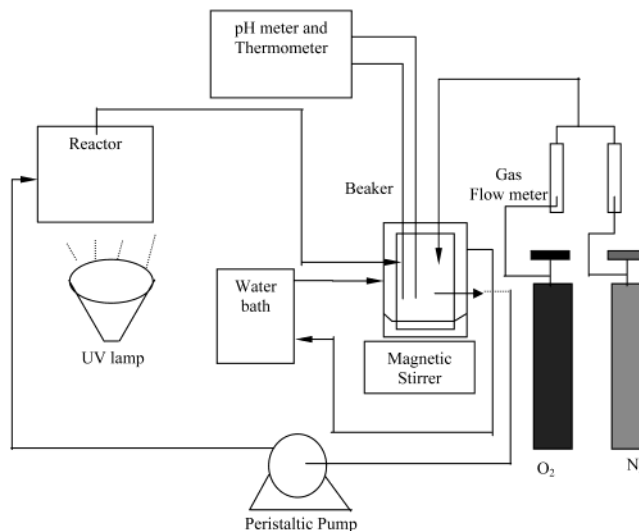


**Figure 1.** Schematic diagram showing the experimental setup.

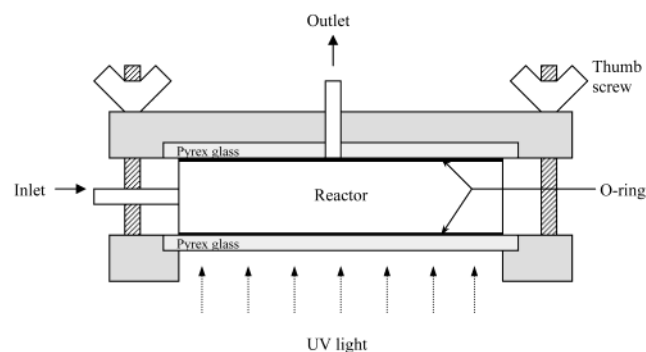


**Figure 2.** Schematic diagram of the monolithic swirl-flow photocatalytic reactor.

analyze the TOC in samples. The concentration of benzoic acid in the reaction samples was analyzed by a high-performance liquid chromatograph (Perkin-Elmer LC240). Aliquots of  $20 \mu\text{L}$  were injected onto a reverse-phase C-18 column (Chrompack) and eluted with a mixture of acetonitrile (60%) and ultrapure water (40%) at a total flow rate of 1.5 mL/min. An absorbance at 229 nm was used to measure the concentration of the above compounds by a UV/vis detector (Perkin-Elmer 785A). All water samples were filtered by a Millex-HA filter (Millipore,  $0.45 \mu\text{m}$ ) before analyses.

**Experimental Procedure.** The experiments were conducted at a low initial substrate concentration (5–30 ppm). A measuring flask was used to prepare the solution with a target concentration of the pollutant, and then the solution along with the required amount of catalyst was poured into the jacketed beaker. The pH of the solution was left as it was; no buffer or other agents were added to control the pH. The total volume of the solution used was always 250 mL. The aqueous solution containing  $\text{TiO}_2$  and the pollutant was introduced tangentially into the reactor by a peristaltic pump from a beaker with a water jacket and exited from the center of the top plate through an outlet plastic tube of 5 mm diameter. The tangential introduction of the solution produced a swirl flow to mix the solution well, thereby reducing the external mass-transfer limitation of the organic substrates from the bulk solution to the catalyst surface. A magnetic stirrer also mixed the solution in the beaker during the entire reaction period. Before turning on the light, the solution was circulated

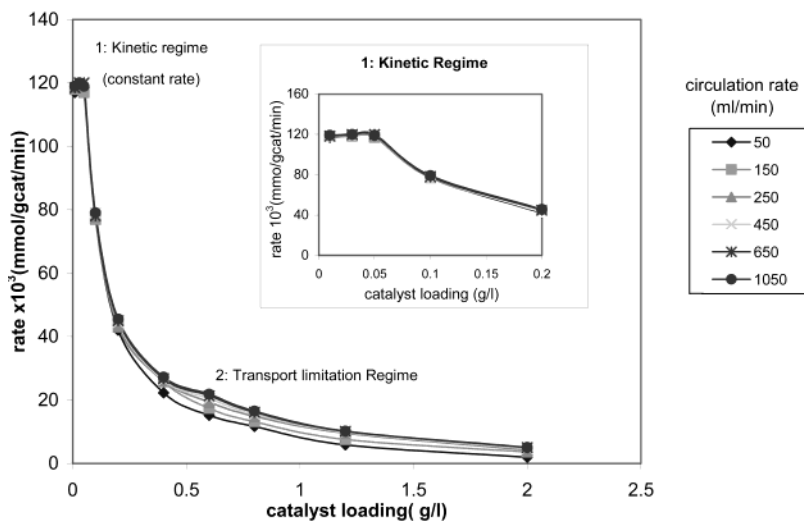


**Figure 3.** Degradation rate (mmol/g of catalyst/min) of benzoic acid for different catalyst loadings showing the kinetic regime. [Experimental conditions:  $C_{S0} = 0.2$  mM,  $\text{pH} = 3.7\text{--}3.9$ ,  $T = 303$  K,  $I = 9.90$  mW/cm<sup>2</sup>, and  $\text{O}_2$  saturated.]

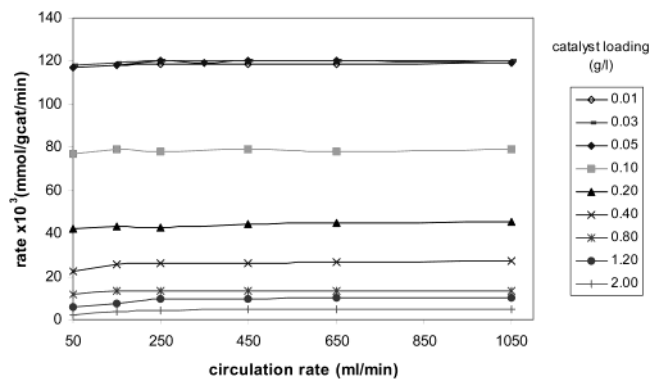


**Figure 4.** Degradation rate (mmol/g of catalyst/min) of benzoic acid against circulation rates at different catalyst loadings. [Experimental conditions:  $C_{S0} = 0.2$  mM,  $\text{pH} = 3.7\text{--}3.9$ ,  $T = 303$  K,  $I = 9.90$  mW/cm<sup>2</sup>, and  $\text{O}_2$  saturated.]

for about 30 min to ensure that the adsorption equilibrium of the pollutant (benzoic acid) had reached the  $\text{TiO}_2$  surface.<sup>43</sup> Oxygen was introduced into the solution continuously to keep the concentration of oxygen constant throughout the reaction. The flow rate of oxygen was measured by a gas flowmeter (model P-200-UO, Tokyo Keiso, Japan). During each run, samples were taken from the beaker at suitable time intervals. Samples of benzoic acid were analyzed using a UV spectrophotometer (UV-1601 PC; Shimadzu). It is worth noting that the catalyst particles were removed from the sample before analysis. In our study, syringe-driven filters (Millex-HA,  $0.45 \mu\text{m}$ ) were used to remove the catalyst particles. All experiments were repeated a few times, and experimental errors for the data reported are within 5%.

## Results and Discussion

**Effect of Catalyst Loading and Circulation Rate.**  
**(a) Rate of Catalytic Transformation (Rate as Mole per Mass of Catalyst per Time).** Figure 3 represents experimental data of the photocatalytic degradation rate of benzoic acid for different catalyst loadings while Figure 4 represents rate versus circulation rate. The experimental studies have been done with catalyst loadings in the range of  $0.01\text{--}2.0$  g/L and at circulation

rates between 50 and 1050 mL/min. The figure reveals that the degradation rate is almost constant (independent of the catalyst loading) for catalyst loadings between 0.01 and 0.05 g/L. The rate then drops gradually as the catalyst loading is increased from 0.05 to 2.0 g/L. The rate is not affected by the circulation rate at the same catalyst loading, but the magnitude of rates with respect to circulation rates is different at different catalyst loadings. Clearly, Figure 3 depicts the kinetic regime for catalyst loadings between 0.01 and 0.05 g/L. In this range, the overall rate is solely controlled by kinetics because when we double the amount of catalyst (in g of catalyst), the conversion (in mmol/min) also doubles; thereby, the resultant rate (in mmol/g of catalyst/min) remains constant. When the catalyst loading is increased above 0.05 g/L, the rate decreases gradually. Hence, in this region, the overall rate is not controlled entirely by kinetics and must be influenced by the transport of either pollutant or light to the catalyst surface. In this transport-limited region, the conversion increases at a slower rate than the increase of the amount of catalyst and, thereby, the overall rate decreases instead of remaining constant as in the kinetic regime. In other words, in this region conversion is influenced by different factors: (a) all of the additional catalyst surface area does not come in contact with a pollutant because of external mass-transfer resistance, (b) the pollutant cannot reach some of the catalyst surface area because of agglomeration of the catalyst particles (internal mass-transfer resistance), (c) light cannot reach some of the catalyst surface area because of absorption and scattering (shielding effect) of light, (d) light cannot penetrate the agglomerates and activate the inner surfaces, and/or (e) a combination of all of the above. Thus, Figure 3 reveals two regimes: (1) the kinetic regime at the low catalyst range ( $<0.05$  g/L) and (2) the transport (mass or light) limitation regime at the high catalyst loading ( $0.05\text{--}2.0$  g/L). In the transport limitation regime, the problem lies in understanding the factor responsible for the limitation.

Figure 4 reveals that the overall reaction rate remains constant with an increase of the circulation rate at any particular catalyst loading. Such results corresponding to the experimental data obtained previously mean that there is no external mass-transfer limitation under the experimental conditions. A qualitative comparison be-

**Table 2. Qualitative Comparison of the Results of Previous Studies Reported in the Open Literature with the Present Work**

investigators	reactor type and capacity, mL	catalyst loading (g/L)	type of circulation				distinguished kinetic and transport limitation regime (yes/no)
			internal stirring yes/no	external circulation			
				yes/no	circulation rate (mL/min)	residence time (s)	
Truchi and Ollis <sup>42</sup>	semibatch, 300 mL	0.027–2.5	yes	yes	not reported		no
Wei and Wan <sup>41</sup>	batch reactor, 1000 mL	0.5–3.0	yes	no	not reported		no
Lakshmi et al. <sup>40</sup>	batch reactor, 75 mL	0.04–0.4	yes	no	not reported		no
Stafford et al. <sup>33</sup>	batch reactor, 800 mL	0.025–1.0	yes	no	not reported		no
Rideh et al. <sup>26</sup>	batch reactor, 2000 mL	0.012–0.2	yes	yes	852	142	no
present work	semibatch, 63.5 mL	0.0125–2.0	yes	yes	350	11	yes

tween data taken from the previous studies and our present work has been presented in Table 2. The specific features related to our experiments are the small volume of the reactor (63.5 mL), low residence time (11 s), internal stirring, and small catalyst loading (0.0125–0.05 g/L). The difference is evident because our results clearly distinguish data related to the kinetic regime. To analyze the cause of such a discrepancy in more detail, a special experiment was performed. A beaker containing 70 mL of the slurry mixture of 0.2 mM benzoic acid and a desired amount of the TiO<sub>2</sub> catalyst was taken. The mixture was stirred in the dark for 0.5 h to allow for adsorption (dark reaction) of benzoic acid on the catalyst surface to reach equilibrium. The beaker was then placed over a glass plate with a UV lamp underneath. The reaction mixture was bubbled with oxygen and stirred very slowly. The resultant initial rate at different catalyst loadings is shown in Figure 5.

When typical rate dependences on the catalyst loading from the previous studies mentioned in Table 2 are compared with results reported in Figures 3 and 5, it can be concluded that at very slow internal stirring high residence time and the absence of external circulation (conditions in Figure 5) diminish the region of rate constancy and under certain conditions the kinetic regime could not be observed. Hence, proper mixing, small catalyst loading, small volume of the reactor, and low residence time, which are characteristics of our experiments shown in Figure 3, are the necessary conditions to obtain data for the well-distinguished kinetic regime. The residence time distribution data and the computational fluid dynamics simulation for the flow characterization of the reactor used in this study are reported elsewhere.<sup>2</sup>

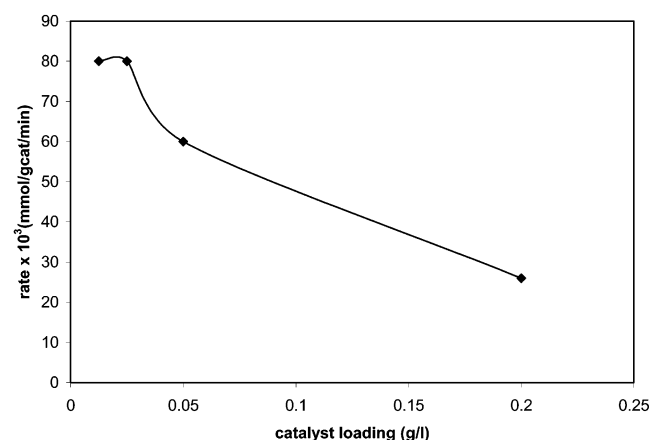


**Figure 5.** Degradation rate (mmol/g of catalyst/min) of benzoic acid for different catalyst loadings without external circulation. [Experimental conditions:  $C_{S0} = 0.2$  mM, pH = 3.7–3.9;  $T = 303$  K,  $I = 8.0$  mW/cm<sup>2</sup>, and O<sub>2</sub> saturated.]

**(b) Apparent Rate of Reaction (Rate as Mole per Volume of Solution per Time).** To analyze the transport (mass or light) limitation regime in more detail, we are representing in Figure 6 the same experimental results of the apparent rate reported in Figures 3 and 4 using another dimension of millimoles per liter of solution per minute, which is most commonly used in the open literature by researchers working in photocatalysis. Figure 6 shows three different domains: (a) the increase of the rate at the low catalyst loading, (b) the constancy of the rate at the intermediate catalyst loading (“optimal catalyst loading” domain), and (c) the decrease of the rate at the high catalyst loading.

This plateau in the optimal loading (working regime) domain becomes smaller and even insignificant with an increase of the circulation rate. We have already seen in Figure 4 that external mass transfer is negligible because the rate (in millimoles per gram of catalyst per minute) was not affected by the circulation rate at any given catalyst loading. When the same experimental data are plotted in Figure 6, it shows that, as we increase the circulation rate, the plateau of constant rate (in millimoles per liter of solution per minute) not only diminishes but also shifts toward higher catalyst loading. Obviously, the circulation rate changes the transport rate, but it is not a case of the external transport limitation. It is very likely that in this region (catalyst loadings between 0.4 and 0.85 g/L) the circulation rate influences agglomeration of catalyst particles. Internal mass-transfer resistance caused by the agglomerate primarily controls the degradation rate. At higher circulation rates, the average size of agglomerated catalyst particles decreases and, therefore, the observed degradation rate increases. Another important aspect to note is the difference between pure kinetic regime values and values corresponding to the optimal catalyst loading regime. There is a significant difference between these rates, and such a difference has not been

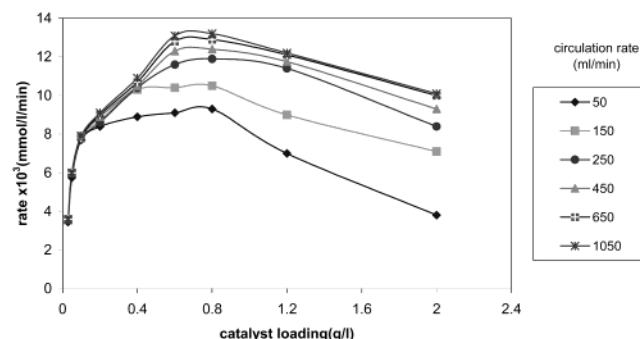


**Figure 6.** Degradation rate (mmol/L of solution/min) of benzoic acid against catalyst loadings at different circulation rates. [Experimental conditions:  $C_{S0} = 0.2$  mM, pH = 3.7–3.9;  $T = 303$  K,  $I = 9.90$  mW/cm<sup>2</sup>, and O<sub>2</sub> saturated.]

presented in the previous studies (e.g., refs 11, 23, 26, and 27). The ratio of the rate at optimal catalyst loading to the rate in the kinetic regime can be estimated as about 0.166 irrespective of the circulation rate using the dimension of rate as millimoles per gram of catalyst per minute (see Figure 4) for an optimal catalyst loading of 0.8 g/L (see Figure 6).

The three factors that can be considered to be responsible for the transport limitation of the overall rate can be distinguished as the following: (a) an increase of the catalyst loading per unit solution volume causes an increase of the apparent rate, while a combination of (b) the mutual influence of a particle (agglomeration of particles) hindering the organic substance to reach the catalyst surface and (c) the ability of photons to penetrate agglomerates and activate the inner surfaces causes a decrease of the apparent rate. The first and the last two factors compensate each other in the second region (domain), resulting in a region of optimal catalyst loading. When the catalyst loading is increased further, the third factor dominates, thus reducing the apparent rate, which Figure 6 clearly demonstrates.

The reasonable explanation of the optimal catalyst loading regime is the appearance of the particle agglomerate under some sufficient catalyst loading. Such a phenomenon of agglomeration for TiO<sub>2</sub> has been reported elsewhere.<sup>35,36</sup> In ref 35, this phenomenon has been observed at the TiO<sub>2</sub> catalyst loading of 10 mg/L, which is even less than our catalyst loading of 50 mg/L.

Generally, the limitation domain can be interpreted as the internal diffusion region, in which the agglomerate plays the role of the porous particle. An estimation of such an agglomerate size can be easily done using the known theoretical relationship for the Thiele modulus,<sup>37</sup> according to which the effectiveness factor  $\eta$  is given by the following equation:

$$\eta = \frac{3}{R} \sqrt{\frac{D_e}{k\rho_p S_a}} \quad (1)$$

where  $k$  is the kinetic constant,  $D_e$  is the diffusion coefficient, and  $R$  is the radius of the agglomerate. The value of the kinetic rate constant can be obtained using the rate value in the kinetic regime of  $\approx 4 \times 10^{-3}$  mmol/L of solution/min (see Figure 6) with initial concentration  $C_{S0} = 0.2$  mmol/L of solution and the specific surface area of the reactor as  $100 \text{ m}^2/\text{m}^3$ . Using the above values, the degradation rate constant  $k$  for benzoic acid is equal to  $3.33 \times 10^{-6}$  m/s, which is of the same order of magnitude as that reported in refs 38 and 39. In the optimal catalyst loading domain,  $\eta = 0.166$ ,  $D_e = 1 \times 10^{-10} \text{ m}^2/\text{s}$ ,<sup>39</sup>  $\rho_p = 2.4 \text{ g}/\text{cm}^3$ , and  $S_a = 50 \text{ m}^2/\text{g}$ ; therefore, the characteristic size of the agglomerate,  $R$ , is given by

$$R = \frac{3}{\eta} \sqrt{\frac{D_e}{k\rho_p S_a}} = 9 \text{ } \mu\text{m} \quad (2)$$

The agglomerate size is in close agreement with data obtained independently and reported elsewhere<sup>16</sup> compared to the average primary particle size of Degussa P25 as 30 nm.

When the catalyst loading is increased even further (greater than 1.2 g/L), the overall rate is limited

primarily by the limitation of transport of light to the catalyst surface, which is described in the literature as the shielding effect. In this region, the addition of further catalyst is like adding inert materials and, therefore, is meaningless. The most important point to note is that constancy of the rate while expressing rate data as moles per mass of catalyst per time reveals the kinetic region, whereas constancy of the rate data when the rate is expressed as moles per volume of solution per time reveals the region of optimal catalyst loading. The determination of all three regions is important and is possible by representing the same set of experimental data in two different rate dimensions. Intrinsic kinetics can be obtained from the kinetic region, which is necessary for catalyst characterization and reactor design. The optimal catalyst loading region is essential from a practical application point of view, while the shielding region states that there is no point in adding any more catalyst, which acts as an inert instead of acting as a catalyst.

**Effect of the Circulation Rate on Adsorption (Dark Reaction) of Benzoic Acid on TiO<sub>2</sub>.** The effect of the circulation rate on the adsorption (dark reaction) of benzoic acid in the range of 50–450 mL/min has been studied to analyze whether the process of dark adsorption is a part of the complex photocatalysis process. It was observed that the rate of dark adsorption remained constant with a change of the circulation rate. The dark adsorption rate in the kinetic regime was found to be 8 mmol/g of catalyst/min, which is much smaller than the complex photocatalytic degradation rate of 120 mmol/g of catalyst/min when experiments were conducted starting with the same initial concentration of benzoic acid. It is therefore evident that the only adsorption (with no illumination) could not remove benzoic acid from the bulk solution. Hence, it is unlikely that the adsorption of benzoic acid on the catalyst surface, which has not been activated by light, plays any significant role in the overall reaction.

**Effect of the Initial Concentration and Light Intensity on the Photocatalytic Degradation Rate in the Kinetic Regime.** It is obvious that the light intensity has a great effect on the photocatalytic reaction rate. In addition, the light intensity may be attenuated because of absorption by the reaction solution. To determine the intrinsic kinetic rate constant, a series of experiments were conducted at different light intensities and initial substrate concentrations in the kinetic regime (catalyst loading of 0.03 g/L), and the concentration–time plots are shown in Figure 7. The results clearly show a first-order rate dependence in the concentration range (<0.30 mM) experiments conducted. Therefore, the rate can be described by the following equation:

$$-dC/dt = k(I) C \quad (3)$$

where  $k$  is the reaction rate constant, which is a function of the incident light intensity. The combined effect of the initial substrate concentration and light intensity on the photocatalytic degradation rate (the slope of the lines in Figure 7) is illustrated in Figure 8 in the kinetic regime.

Figure 8 shows that the rate increases sharply initially with an increase of the light intensity, and then the rise becomes less gradual. Qualitatively, at the domain of high initial concentration, these results are similar to those previously reported in refs 27, 29, and

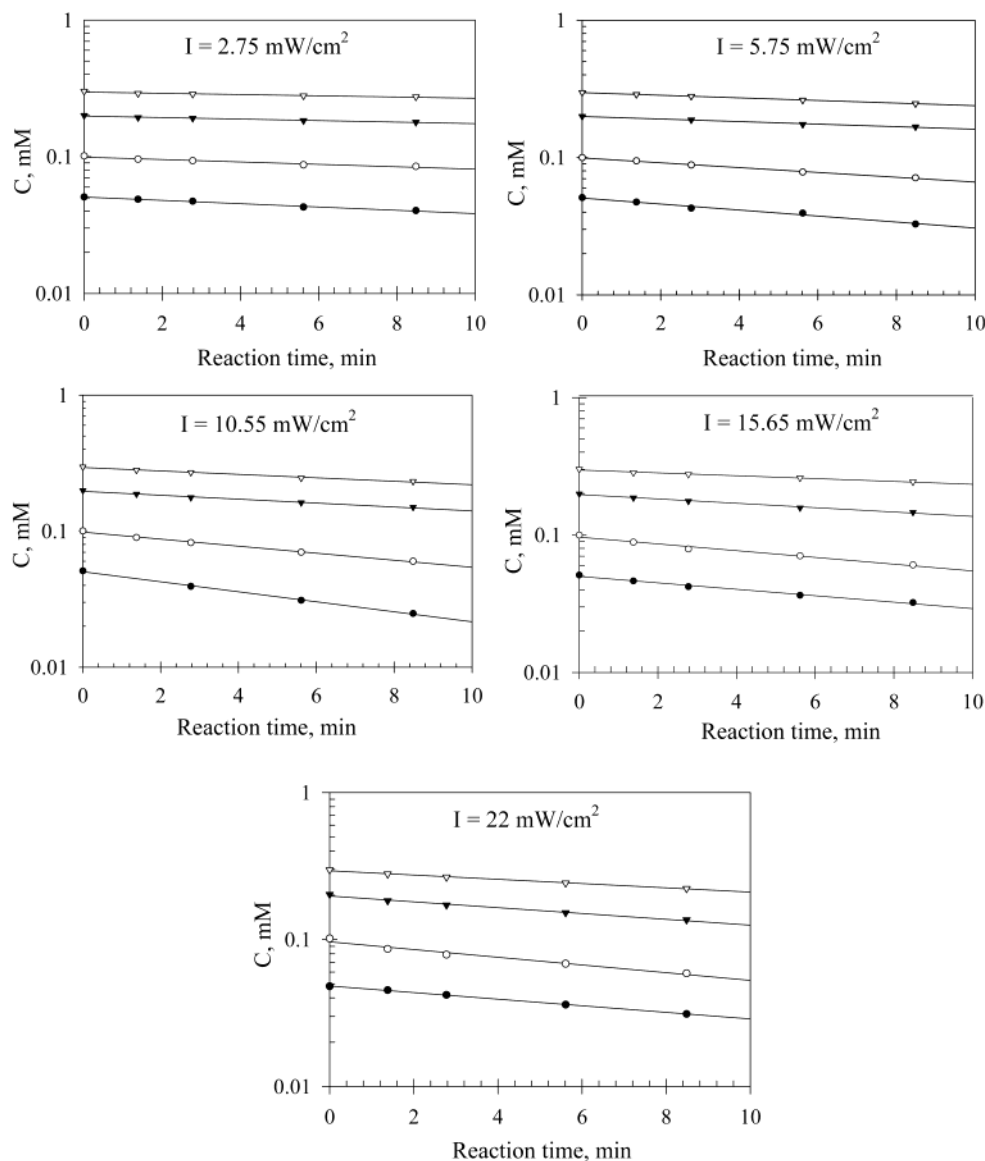


**Figure 7.** Degradation of benzoic acid at different light intensities and initial substrate concentrations in the kinetic regime. [Experimental conditions: catalyst loading = 0.03 g/L, circulation rate = 350 mL/min, pH = 3.7–3.9,  $T = 303$  K,  $O_2$  saturated.]

34 for the photocatalytic degradation of other organic compounds. In photocatalysis literature, the dependence of the degradation rate constant ( $k$ ) is usually described by

$$k = aI^\beta \quad (4)$$

where  $I$  is the light intensity at the catalyst surface,  $a$  is a proportionality constant, and  $\beta$  is a kinetic order. Because the reaction liquid attenuates the light intensity, the above equation can be modified as

$$k = a[I_0 \exp(-b'C)]^\beta = a \exp(-bC^n) I_0^\beta \quad (5)$$

where  $I_0$  is the incident light intensity used in the experiments and  $b$ ,  $b'$ , and  $n$  are constants. The constants  $b$  and  $b'$  are light absorption coefficients by the reaction liquid. By using a nonlinear optimization routine, we found that the above equation fits very well for all of the data shown in Figure 8. When the values of  $k$ ,  $I_0$ , and  $C$  are expressed as  $s^{-1}$ ,  $mW/cm^2$ , and mM, the values obtained for the constants  $a$  and  $b$  are 25.13

and 2.47, respectively, while the kinetic orders  $n$  and  $\beta$  obtained are 0.5 and 0.333, respectively.

**Effect of the Light Intensity and Catalyst Loading on the Degradation Rate.** The combined effect of the light intensity and catalyst loading on the photocatalytic degradation rate of benzoic acid is shown in Figure 9 in the transport-limited (mass- or light-limiting) regime. Experiments were done to determine the combined effect of the two parameters when the catalyst loading was varied between 0.4 and 2.5 g/L while the range of light intensity used was between 1 and 22  $mW/cm^2$ . Sections of Figure 9 have been shown as Figure 10, depicting the effect of the catalyst loading on the degradation rate at different light intensities. In Figures 9 and 10, the rate is plotted in units of mmoles per volume of solution per time because we are in the transport-limited region. We have already seen that in this region there is no external mass-transfer resistance (see Figure 4) and the average agglomerate size of catalyst particles is 9  $\mu m$ . Figure 10 clearly shows that at any particular light intensity the rate is almost constant when the catalyst loading is greater than 1.25 g/L. However, the rate increases with an increase of the

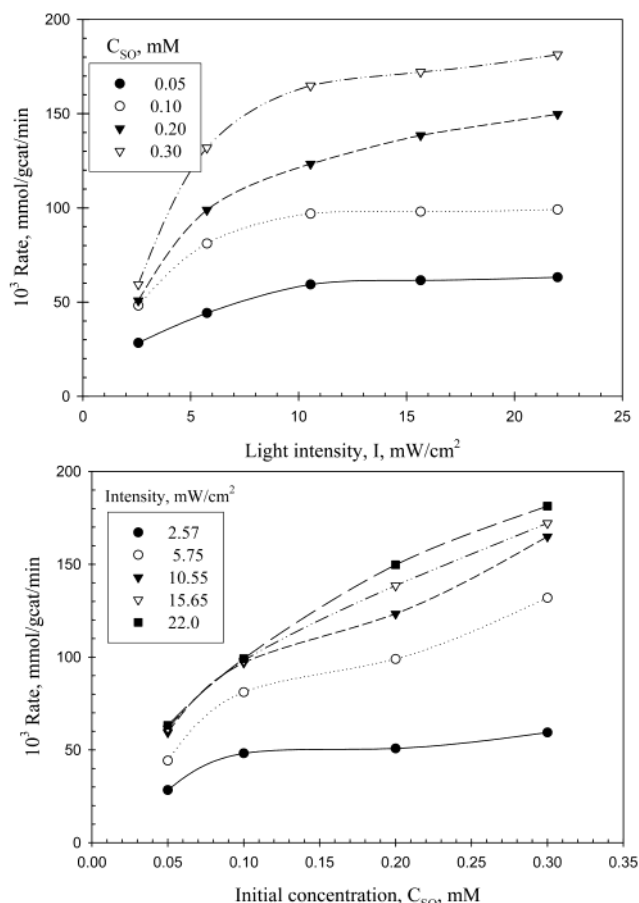


**Figure 8.** Degradation rate as functions of the light intensity and initial substrate concentration in the kinetic regime. [Experimental conditions: catalyst loading = 0.03 g/L, circulation rate = 350 mL/min, pH = 3.7–3.9,  $T = 303$  K, O<sub>2</sub> saturated.]

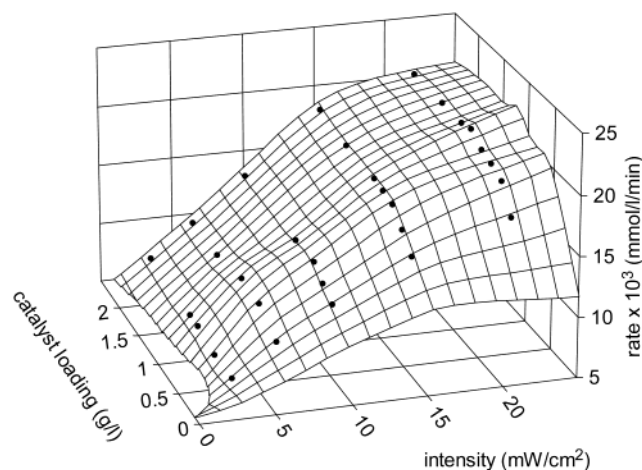


**Figure 9.** 3D plot of the degradation rate (mmol/L of solution/min) against light intensity and catalyst loading. [Experimental conditions:  $C_{SO} = 0.2$  mM, pH = 3.7–3.9,  $T = 303$  K, O<sub>2</sub> saturated,  $Q = 350$  mL/min.]

light intensity at any given catalyst loading. In the low catalyst loading region (0.5–1.25 g/L), there is “hindered transport” of the organic substance to the catalyst surface due to agglomeration, while in the high catalyst loading region (>1.25 g/L), there is a “shielding effect” because the catalyst loading certainly creates an obstacle for the transport of light to the catalyst surface. In this region, the addition of catalyst loading is like adding inert materials to the system. When the rate (in

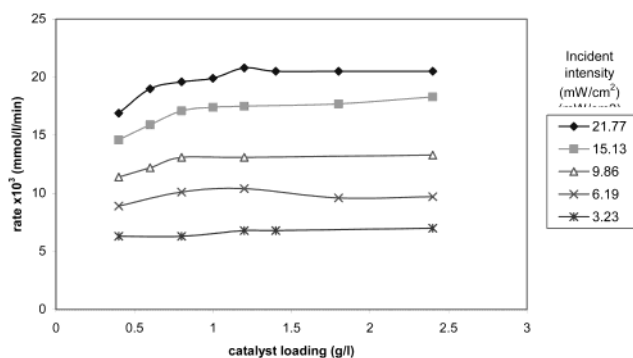


**Figure 10.** Degradation rate (mmol/L of solution/min) against catalyst loading at different light intensities. [Experimental conditions:  $C_{SO} = 0.2$  mM, pH = 3.7–3.9,  $T = 303$  K, O<sub>2</sub> saturated,  $Q = 350$  mL/min.]

mmoles per liter of solution per minute) at the high catalyst loading region (>1.25 g/L) was fitted to the equation

$$-dC/dt = R = k_{\text{obs}}C = aI^{\beta}C \quad (6)$$

the value of kinetic order,  $\beta$ , obtained was 0.58, which is in contrast to the value obtained earlier ( $\beta = 0.33$ ) in the kinetic regime. Although our analysis could distinguish between the kinetic regime and the optimal catalyst loading regime, it is difficult to distinguish between the internal mass-transfer limitation regime and the shielding effect regime. It appears that the latter two regimes are overlapping. It is to be noted that the shielding effect is not only due to the inability of photons to penetrate the agglomerates and activate the inner surfaces but also due to the presence of other agglomerates in the solution. In this paper, we have not elaborated about the mechanism of the photocatalytic process and also have not presented data related to the detailed influence of some other parameters, such as pH, temperature, etc., on the degradation rate. It will be a part of our future studies and will be presented later.

## Conclusions

Systematic kinetic studies of parameter influence (catalyst loading, circulation rate, substance initial concentration, and light intensity) on the reaction rate of photocatalytic degradation of benzoic acid in TiO<sub>2</sub> slurry systems have been presented in this paper. Operating with the data “reaction rate versus catalyst loading”, we observed that when the rate data are plotted per unit mass of catalyst, one could identify the kinetic region from the constancy of the rate data. In contrast, when the same experimental data were plotted with the rate data expressed as per unit volume of reaction liquid, one could identify the region of optimal catalyst loading from the constancy of the rate data, where the rate is limited primarily by internal mass transfer due to agglomeration of catalyst particles. The kinetic limitation domain occurs at low catalyst loading, and intrinsic (true) kinetic dependences, particularly the “reaction rate–light intensity” dependence, were determined, which can only be obtained from the data in the kinetic region. The optimal catalyst loading domain is a distinctive part of the transport limitation domain (which occurs at intermediate values of the catalyst loading and is a general feature of the multiphase catalytic process), in which the reaction rate is likely

governed by transport processes within the catalyst particle agglomerate (estimated size of the agglomerate was found to be 9  $\mu\text{m}$ ), i.e., internal mass transport limitation. It was observed that, in the optimal catalyst loading region, there is no external mass transport limitation, but the circulation rate influences agglomeration of catalyst particles as the rate plateau shifts toward higher values of catalyst loading when the circulation rate is increased. A significant difference in the rate values between the optimal catalyst loading regime and the kinetic regime was observed. Determination of this region is very important because one can readily obtain from the kinetic regime the intrinsic reaction rate constant, which is required for catalyst characterization, elucidation of the mechanism of the photocatalytic reaction, and in the reactor design, while determination of optimal catalyst loading is important for practical applications. It is, however, difficult to distinctively distinguish the internal mass-transfer limitation regime and the shielding effect domain because they are most likely overlapping. The kinetic order on the light intensity was found to be 0.33 in the kinetic regime, while it is 0.58 in the primarily shielding effect region. The analysis presented in this work for the slurry system can be used for any heterogeneous catalysis systems.

### Notation

$\beta$  = kinetic order  
 $C_{S0}$  = initial concentration of the substrate, mM  
 $D_e$  = diffusion coefficient,  $\text{cm}^2/\text{s}$   
 $I$  = incident light intensity,  $\text{mW}/\text{cm}^2$   
 $k$  = reaction rate constant,  $\text{s}^{-1}$   
 $L$  = agglomerate size, mm  
 $\eta$  = effectiveness factor  
 $P_{O_2}$  = partial pressure of oxygen, atm  
 $Q$  = circulation rate, mL/min  
 $R$  = rate, mmol/l of solution/min or mmol/g of catalyst/min  
 $T$  = temperature, K  
 $w$  = catalyst loading, g/L

### Literature Cited

- (1) Bard, A. J. *Science* **1980**, *207*, 139.
- (2) Ray, A. K.; Beenackers, A. A. C. M. *AIChE J.* **1997**, *43*, 2571.
- (3) Peiró, A. M.; Ayllón, J. A.; Peral, J.; Doménech, X. *Appl. Catal. B* **2001**, *30*, 359.
- (4) Pruden, A. L.; Ollis, D. F. *Environ. Sci. Technol.* **1983**, *17*, 628.
- (5) Pruden, A. L.; Ollis, D. F. *J. Catal.* **1983**, *82*, 404.
- (6) Hsiao, C. Y.; Lee, C. L.; Ollis, D. F. *J. Catal.* **1983**, *83*, 418.
- (7) Ollis, D. F.; Hsiao, C. Y.; Budiman, L.; Lee, C. L. *J. Catal.* **1984**, *88*, 89.
- (8) Okamoto, K.; Yamamoto, Y.; Tanaka, H.; Itaya, A. *Bull. Chem. Soc. Jpn.* **1985**, *58*, 2023.
- (9) Matthews, R. W. *J. Phys. Chem.* **1987**, *91*, 3328.
- (10) Matthews, R. W. *J. Catal.* **1988**, *111*, 264.
- (11) Matthews, R. W. *Water Res.* **1990**, *24* (5), 663.
- (12) Mills, A.; Morris, S. *J. Photochem. Photobiol., A* **1993**, *71*, 75.
- (13) Mills, A.; Davies, R. H.; Worsley, D. *Chem. Soc. Rev.* **1993**, *417*.
- (14) Legrini, O.; Oliveros, E.; Braun, A. M. *Chem. Rev.* **1993**, *93*, 671.
- (15) Fox, M. A.; Dulay, M. T. *Chem. Rev.* **1993**, *93*, 341.
- (16) Hoffman, M. R.; Martin, S. T.; Choi, W.; Bahnemann, D. W. *Chem. Rev.* **1995**, *95*, 69.
- (17) Mills, A.; Le Hunte, S. *J. Photochem. Photobiol., A* **1997**, *108*, 1.
- (18) Blake, D. M. *Bibliography of work on Photocatalytic Removal of Hazardous Compounds from Water and Air*; NREL/TP-430-22197; National Renewable Energy Laboratory: Golden, CO, 1997.
- (19) Herrmann, J. *Catal. Today* **1999**, *53*, 115.
- (20) Serpone, N.; Pelizzetti, E., Eds. *Photocatalysis: Fundamentals and Application*; Wiley: New York, 1989.
- (21) Schiavello, M., Ed. *Photocatalysis and Environment Trends and Applications*; Kluwer Academic Publishers: Dordrecht, The Netherlands, 1988.
- (22) Schivello, M., Ed. *Heterogeneous Photocatalysis*; John Wiley & Sons: Chichester, U.K., 1997; Vol. 3.
- (23) Inel, Y.; Okte, A. N. *J. Photochem. Photobiol., A* **1996**, *96*, 175.
- (24) Turchi, C. S.; Ollis, D. F. *J. Catal.* **1990**, *122*, 178.
- (25) Matthews, R. W. *Water Res.* **1990**, *24*, 5, 653.
- (26) Rideh, L.; Wehrer, A.; Ronze, D.; Zoulalian, A. *Ind. Eng. Chem. Res.* **1997**, *36*, 4712.
- (27) Chen, D.; Ray, A. K. *Water Res.* **1998**, *32* (11), 3223.
- (28) Palmisano, L.; Scalfani, A. In *Heterogeneous Photocatalysis*; John Wiley & Sons: Chichester, U.K., 1997.
- (29) D'Oliveira, J.; Al-Sayyed, G.; Pichat, P. *Environ. Sci. Technol.* **1990**, *24*, 990.
- (30) Augugliaro, V.; Lopez-Munoz, M. J.; Palmisano, L.; Soria, J. *Appl. Catal., A* **1993**, *101*, 7.
- (31) Chen, L.; Chou, T. *Ind. Eng. Chem. Res.* **1993**, *32*, 1520.
- (32) Stefoglo, E. F. *Chem. Eng. Commun.* **1986**, *41*, 327.
- (33) Stafford, U.; Gray, K. A.; Kamat, P. V. *J. Catal.* **1997**, *167*, 25.
- (34) Al-Sayyed, G.; D'Oliveira, J. C.; Pichat, P. *J. Photochem. Photobiol., A* **1991**, *58*, 99.
- (35) O'Shea, K. E.; Pernas, E.; Saires, J. *Langmuir* **1999**, *15*, 2071.
- (36) Chen, H. Y.; Zahraa, O.; Bouchy, M.; Thomas, F.; Bottero, J. Y. *J. Photochem. Photobiol., A* **1995**, *85*, 179.
- (37) Levenspiel, O. *Chemical Reaction Engineering*, 3rd ed.; John Wiley & Sons: New York, 1991; p 391.
- (38) Matthews, R. W. *J. Phys. Chem.* **1987**, *91*, 3328.
- (39) Chen, D.; Li, F.; Ray, A. K. *Catal. Today* **2001**, *66*, 475.
- (40) Lakshmi, S.; Renganathan, R.; Fujita, S. *J. Photochem. Photobiol., A* **1995**, *88*, 163.
- (41) Wei, T. Y.; Wan, C. C. *Ind. Eng. Chem. Res.* **1991**, *30*, 1293.
- (42) Turchi, C. S.; Ollis, D. F. *J. Catal.* **1989**, *119*, 483.
- (43) Chen, D. W.; Li, F.; Ray, A. K. *AIChE J.* **2000**, *46*, 1034.

Received for review December 9, 2002

Revised manuscript received March 28, 2003

Accepted March 28, 2003

IE0209881